PCCP

ROYAL SOCIETY OF CHEMISTRY

PAPER

View Article Online
View Journal | View Issue

Cite this: *Phys. Chem. Chem. Phys.*, 2024, **26**, 11379

Determining the quantum yield of photochemical reactions in crystals from simultaneous effects of photothermal and photochemical bending of needle-shaped crystals

Stanislav Chizhik, * Pavel Gribov, Viktor Kovalskii and Anatoly Sidelnikov

Received 8th February 2024,
Accepted 21st March 2024

DOI: 10.1039/d4cp00581c

rsc.li/pccp

Photoinduced bending of needle crystals caused by photochemical transformation can be used as an extremely sensitive method for studying the kinetics of the transformation. However, the determination of the absolute value of the quantum yield of the reaction requires an accurate value of the intensity of light penetrating the crystal, in contrast to reactions in solutions where only the value of the total absorbed irradiation dose is sufficient. To address this problem, this study utilizes the effect of photothermal bending of a crystal due to its heating by light, occurring simultaneously with the bending due to transformation and proportional to the same value of light intensity. The ratio of the amplitudes of the two effects is independent of the light intensity, which allows the quantum yield to be determined without knowledge of the intensity value. In addition, the method allows the light intensity and thermal conductivity of the crystal to be estimated. The method is applied to measure wavelength dependence of the quantum yield of nitro-to-nitrito photoisomerization in $[Co(NH_3)_5NO_2]Cl(NO_3)$ crystals. A monotonically decreasing value of the quantum yield φ from 0.19 to 0.04 in the range of λ from 403 to 523 nm was obtained. This result indicates the qualitative differences in the transformation mechanism in crystals and in solutions, where φ = 0.03 independent of λ in the same wavelength range.

1 Introduction

In the last decade, interest has grown in the study of dynamic crystal phenomena, which include various dynamic effects like bending, twisting, rapid displacements, and spontaneous destruction caused by phase or chemical transformations initiated by various stimuli such as heating or irradiation of crystals.[1–8] All such phenomena are associated with the occurrence of inhomogeneous strains due to inhomogeneous development of transformations in crystals.[9–12] Photomechanical effects, like bending of thin crystals caused by photoisomerization of the constituent molecules, are the most actively considered phenomena in this field as they can be used to create microactuators controlled by light.[13–17]

But beyond that, these phenomena provide a pathway to new precision methods for studying photochemical reactions in crystals. In those cases where the transformation does not cause structural rearrangement of the crystal, its amorphization or plastic deformation, the transformation is unambiguously related to the resulting deformations, so that the solution of the inverse problem allows us to study the kinetics of transformation with sensitivity inaccessible to other methods.

This method historically originated from the study of photoinduced bending of needle-shaped crystals of $[Co(NH_3)_5NO_2]Cl(NO_3)$, experiencing isomerization in the coordination of cobalt by the ambidentate ligand NO_2^- (from Co–NO_2 to Co–ONO, nitro–nitrito isomerization).[18,19] Further development of the method is able to provide detailed information on the absorption of light by the substance, the spatial distribution of the transformation in the crystal, and the value of the quantum yield, the most important characteristic of the photochemical reaction.[20–23]

However, there are still specific difficulties in determining the quantum yield in solids. In contrast to solutions, where it is sufficient to measure the total absorbed irradiation dose that caused the transformation, in the case of crystals it is necessary to know the light intensity. Without detailed information on the angular intensity distribution of the light source, this can lead to significant errors in the absolute value of the quantum yield determined in various experiments using averaged intensity in the light beam.[20] Therefore, it is very desirable to develop an experimental approach that avoids the need to know the exact value of the light intensity to calculate the quantum yield.

In this study, it is proposed to use for this purpose the photothermal effect arising simultaneously with the transformation – the

Institute of Solid State Chemistry and Mechanochemistry SB RAS, Kutateladze 18, 630128 Novosibirsk, Russia. E-mail: stas@solid.nsc.ru

bending of a crystal due to inhomogeneous heating by the absorbed light.[24] Since both photothermal and photochemical bending of a crystal are proportional to the same light intensity, their ratio does not depend on it and is determined by the ratio of strains caused by transformation and heating. In addition, the method can be used to determine the light intensity itself, as well as the thermal conductivity of the crystal.

Photochemical isomerization in $[Co(NH_3)_5NO_2]Cl(NO_3)$ crystals was used to test the idea. Crystals and solutions of this complex experience the transformation from a thermally stable nitro isomer to a nitrito isomer under irradiation with visible or UV light at $\lambda < 530$ nm. The reverse isomerization occurs spontaneously: in a few days at room temperature, or in a few minutes with heating up to 80 °C.[18–20,25–27] Isomerization in the crystals does not change the initial orthorhombic crystal structure, except for a linear change of lattice parameters with the degree of transformation,[20] which makes it possible to follow the transformation kinetics by measuring the bending of a needle crystal irradiated from one side.

$[Co(NH_3)_5NO_2]X_2$ crystals with various anions (X = Cl, Br, and I) have been investigated earlier in a number of studies,[26–32] but the only mention of the quantum yield measurement in the crystals can be found in a short report in ref. 33, where the quantum yield $\varphi = 0.2 \pm 0.05$ is given without experimental details. Here, we demonstrate the use of the new method to obtain the wavelength dependence of quantum yield for visible light from 403 to 523 nm.

2 Experimental method

To study the dynamics of crystal bending, the displacement of the laser beam reflected from a micromirror (a small silicon plate) glued to the end of a cantilevered crystal was tracked (Fig. 1). Crystals with a length of 5–13 mm and a thickness of 180–280 μm were used.

Collimated irradiation from 1 W LEDs (λ = 403 nm, 465 nm, 523 nm) and a 100 W xenon arc lamp with bandpass interference filters (405 nm, 425 nm, 436 nm, 461 nm, 491 nm) was used as the light source. A mechanical shutter was used to control the exposure periods.

The movement of the laser spot along the measuring template located at a distance of about 2 m from the crystal was recorded using a 50 fps video camera. The video files were analyzed using in-house developed software based on automatic tracking of the laser spot movement relative to the template marks located at the vertices of a 10 × 10 cm square ("Laser Spot Track" plugin for ImageJ[34] is available at **https://imagej.net/PhotoBend**).

The spatial resolution of the laser spot movement achieved in the experiment was about 50 μm. For a crystal located at a 2 m distance this provides a resolution of 7×10^{-3} deg for the bending angle, or 60 nm deflection of the free end of a 1 cm long crystal. This corresponds to a transverse strain gradient resolution of 10^{-7} per 100 μm of crystal thickness, which can be caused, for example, by a temperature gradient of 10^{-3} K per 100 μm (for a thermal expansion coefficient of 10^{-4} K^{-1}), or by 0.01% transformation in a 10 μm surface layer of such a crystal.

Fig. 2 demonstrates the dynamics of the reflected beam movement as a result of five exposure periods of different durations. Each time, at the onset of irradiation, the crystal experiences a rapid bending with the same amplitude in each cycle, taking a time of about 100 ms. This is followed by a slower curvature growth with the same rate in each cycle, related to the accumulation of the nitrito isomer in the surface layer. At the end of each exposure, a rapid limited unbending occurs, reversed in the direction and taking the same time as the rapid bending phase at the exposure start. Between exposures, the bending achieved due to isomerization does not change, since the rate of reverse isomerization at room temperature is negligible. The described rapid bending and unbending steps correspond to the photothermal effect. Deformations occurring during the establishment and disappearance of the transverse temperature gradient estimated here to be 0.035 K over the crystal thickness of 280 μm. The total transformation degree reached at the surface after five exposures is estimated to be 2.5%.

3 Model

3.1 Photothermal effect

One side of a needle crystal is heated by light due to nonradiative deactivation of photoexcited states appearing in the irradiated surface layer. A flux of quanta I_0 [s^{-1} cm^{-2}] carries an

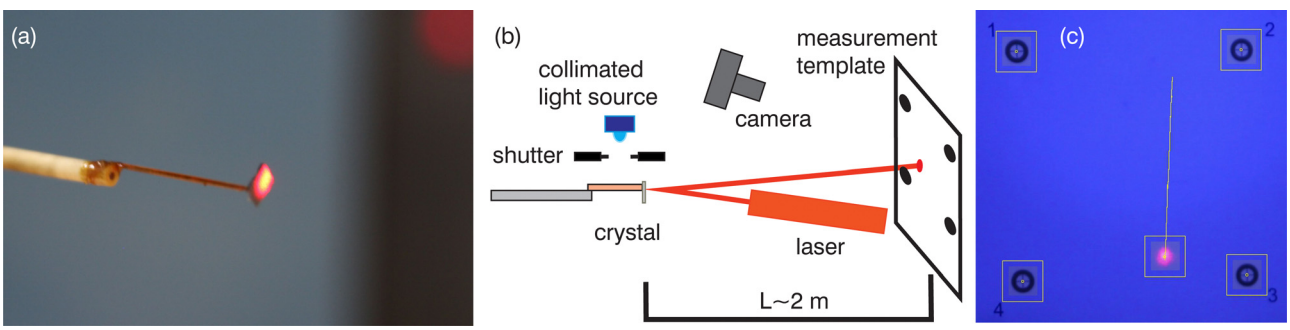

Fig. 1 Experimental setup: a cantilevered crystal (length 13 mm, cross-section 280 × 350 μm) with a Si mirror at the free end (a), scheme of the experimental setup (b), and trajectory of the laser spot movement relative to the template marks (c).

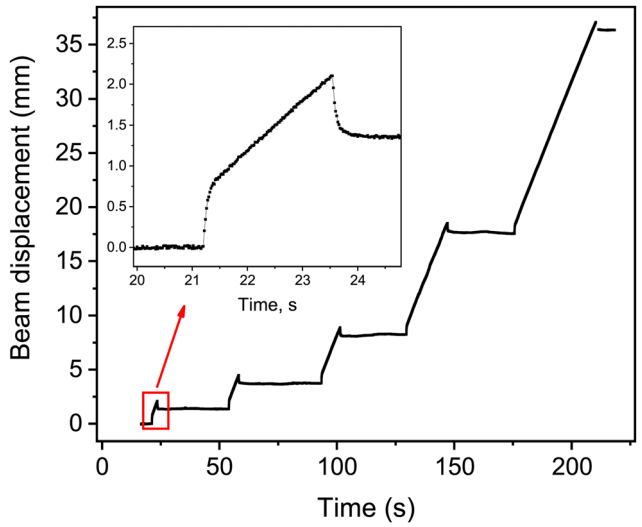

Fig. 2 Displacement of the reflected laser beam as a result of five exposure periods of different durations. Light source: 1 W LED 465 nm; crystal length 13 mm; and cross-section 280 × 350 μm. In the inset – enlarged image of the first exposure period.

energy flux $J_0 = I_0\hbar\omega$ onto the crystal. Absorbed in the surface layer $\sim\mu^{-1}$, this flux provides the bulk heat release $w = J_0\mu e^{-\mu x}$ at depth x of the crystal with the absorption coefficient μ, according to the Bouguer–Beer–Lambert law. The temperature evolution is subject to the heat conduction equation with the volumetric heat release term

$$\frac{\partial T}{\partial t} = D_T \Delta T + \frac{w}{c}, \tag{1}$$

where $D_T = \kappa/c$ is the thermal diffusivity and κ and c are the thermal conductivity and heat capacity of the crystal.

The crystal temperature rise is limited by heat exchange with air at temperature T_0, which can be described using empirical expressions for convective heat exchange of horizontal heated cylinders,[35] and which defines the boundary condition of the problem

$$-\kappa\frac{\partial T}{\partial \mathbf{n}} = \mathrm{Nu}\frac{\kappa_g}{d}(T - T_0), \tag{2}$$

where κ_g is the thermal conductivity of air, d is the effective diameter of the crystal section, and Nu is the Nusselt coefficient estimated here to be Nu = 0.35 according to ref. 35.

An approximate solution of this problem can be obtained by splitting the heat source w into an average part $w_m = J_0(1 - e^{-\mu h})/h$ and a residual $w' = w - w_m$. The latter corresponds to zero total heat release and, therefore, does not lead to the overall heating of the crystal, but only to a temperature inhomogeneity. The average component w_m causes the overall heating of the crystal. Accordingly, the temperature change of the crystal can be represented as $T(r,t) - T_0 = T_m(t) + T'(r,t)$, where $T_m(t)$ is the growth of the average temperature of the crystal, which does not cause its bending and is not important for the considered problem, $T'(r,t)$ is the inhomogeneous component leading to the bending.

Due to the difference between κ and κ_g by more than an order of magnitude, the heat transfer to the gas is predominantly determined by the average crystal temperature T_m, whereas in the problem on T' the heat transfer to the gas can be neglected. Further it will be shown that by the moment when the heat exchange with gas becomes essential, the condition $T' \ll T_m$ is satisfied.

By integrating eqn (1) over the cross-section of the crystal, taking into account the boundary condition (2), and neglecting the inhomogeneity of temperature at the boundary, the following expression for $T_m(t)$ can be obtained.

$$\begin{aligned} T_m &= T_{max}\left(1 - e^{-t/t_m}\right), \\ T_{max} &= \frac{w_m d^2}{4\kappa_g \mathrm{Nu}}, \\ t_m &= \frac{\kappa}{\kappa_g}\frac{d^2}{4D_T\mathrm{Nu}}. \end{aligned} \tag{3}$$

In a typical case with radiation power $J_0 \sim 0.1$ W cm^{-2} absorbed by a 200 μm thick crystal, the maximum temperature rise T_{max} reaches about 5 K.

Since w' depends only on x and the heat exchange with air can be neglected, the problem for T' is formulated as the one-dimensional eqn (4)

$$\frac{\partial T'}{\partial t} = D_T\frac{\partial^2 T'}{\partial x^2} + \frac{w'}{c}. \tag{4}$$

The solution for T' can be obtained as a series

$$T' = \sum_{n=1}^{\infty} a_n v_n(x)[1 - u_n(t)], \tag{5}$$

where functions u_n and v_n are defined by

$$u_n = \exp(-k_n^2 D_T t/h^2), \quad v_n = \cos(k_n x/h), \tag{6}$$

$k_n = \pi n$. Coefficients a_n are

$$a_n = \frac{2J_0 h}{\kappa}\left(\frac{\mu h}{\pi n}\right)^2 \frac{1 - (-1)^n e^{-\mu h}}{(\mu h)^2 + (\pi n)^2}. \tag{7}$$

At $t \to \infty$ the sum of series (5) tends to the function

$$\begin{aligned} T'_\infty(x) = \frac{J_0 h}{\kappa}\Bigg\{&\frac{2 + e^{-\mu h}}{6} - \frac{\mu x + e^{-\mu x}}{\mu h} \\ &+ \left[\frac{1}{2}\left(\frac{x}{h}\right)^2 + \frac{1}{(\mu h)^2}\right]\left(1 - e^{-\mu h}\right)\Bigg\}, \end{aligned} \tag{8}$$

which determines the stationary temperature inhomogeneity achieved in the photothermal effect. Under strong absorption conditions, $\mu h \gg 1$, the maximum temperature difference between opposite crystal surfaces can be achieved as

$$\Delta T'_{max} = \lim_{\mu h\to\infty}\left[T'_\infty(0) - T'_\infty(h)\right] = \frac{J_0 h}{2\kappa}. \tag{9}$$

Comparison with eqn (3) shows that $\Delta T'_{\max}/T_{\max} \sim \kappa_g/\kappa \ll 1$.

As can be seen from (6), characteristic time of the slowest changing term in (5) can be determined using

$$t_c = \frac{h^2}{\pi^2 D_T}. \tag{10}$$

It is this time that determines the characteristic duration of the photothermal bending. Comparison with t_m in (3) shows that the ultimate heating of the crystal takes two orders of magnitude longer than the time required for the establishment of inhomogeneous temperature distribution over the crystal thickness.

Next, the dynamics of the bending moment and curvature of the crystal can be determined from T'. The thermal strain moment is defined by the expression

$$\begin{aligned} M_{th} &= \alpha_T \int_0^h \left(\frac{h}{2} - x\right) T' \mathrm{d}x \\ &= \alpha_T \sum_{n=1}^{\infty} a_n [1 - u_n(t)] \frac{1 + (-1)^{n+1}}{\pi^2 n^2}, \end{aligned} \tag{11}$$

where α_T is the coefficient of thermal expansion along the crystal axis (1.07×10^{-4} K^{-1} at room temperature for the investigated crystals[20]). When evaluating M_{th} it is sufficient to get the value of the first summand only in (11), which reproduces the whole dependence of $M_{th}(t)$ with an error of 1% or better because the coefficients of the series in (11) decrease as, at least, n^{-4}, the characteristic times for u_n decrease as n^{-2}, and only the terms with odd n are non-zero. An even more accurate expression can be obtained if, instead of the coefficient of the first term of the series $2a_1/\pi^2$, we use the exact value of the moment calculated for the function $T'_\infty(x)$.

A strain moment M causes a homogeneous crystal bending characterized by the curvature radius R defined by eqn (12)

$$\frac{1}{R} = \frac{12M}{h^3}. \tag{12}$$

Thus, the curvature caused by the crystal heating changes according to eqn (13)

$$\begin{aligned} \left(\frac{1}{R}\right)_{th} &= \left(\frac{1}{R}\right)_{\infty} \left[1 - \exp\left(-\frac{D_T t}{\pi^2 h^2}\right)\right], \\ \left(\frac{1}{R}\right)_{\infty} &= \frac{\alpha_T J_0}{2\kappa} \\ &\times \left[\left(1 - \frac{12}{(\mu h)^2}\right)\left(1 + \mathrm{e}^{-\mu h}\right) + \frac{24\left(1 - \mathrm{e}^{-\mu h}\right)}{(\mu h)^3}\right]. \end{aligned} \tag{13}$$

It follows from (13) that the values of D_T and κ can be obtained from the kinetics of the photothermal effect. Additionally, with the known α_T and μ, the light intensity penetrating the crystal $I_0 = J_0/\hbar\omega$ can be determined from the amplitude of the photothermal bending. In the case of strong absorption $\mu h \gg 1$, the maximum photothermal bending does not depend on the thickness of the crystal, and is determined only by the intensity of the light and the properties of the substance $R_\infty^{-1} \to \alpha_T J_0/2\kappa$.

A similar consideration of the crystal cooling after turning off the illumination shows that the curvature changes in the opposite way with respect to eqn (13): $R_{th}^{-1} = R_\infty^{-1} \exp(-D_T t/\pi^2 h^2)$.

3.2 Crystal bending by the photoisomerization

Simultaneously with heating, the absorbed light causes photoisomerization. Since the depletion of the initial isomer can be neglected for small degrees of isomerization, the reaction rate can be expressed using the equation

$$\frac{\mathrm{d}C}{\mathrm{d}t} = I_0 \mu \varphi v_0 \mathrm{e}^{-\mu x}, \tag{14}$$

C is the fraction of the photoisomer, φ is the quantum yield, and v_0 is the volume per single molecule. The bending moment due to isomerization is

$$M_{iso} = \varepsilon_0 \int_0^h \left(\frac{h}{2} - x\right) C \mathrm{d}x, \tag{15}$$

ε_0 is the longitudinal strain at complete isomerization (*ca.* 3.4% at room temperature for the substance under consideration[20]). The corresponding rate of curvature increase is

$$\frac{\mathrm{d}}{\mathrm{d}t}\left(\frac{1}{R}\right)_{iso} = \frac{6 I_0 \varphi v_0 \varepsilon_0}{h^2}\left(1 + \mathrm{e}^{-\mu h} - 2\frac{1 - \mathrm{e}^{-\mu h}}{\mu h}\right). \tag{16}$$

3.3 Determination of quantum yield

With the irradiation onset, both processes begin simultaneously. The resulting curvature is determined by the sum of two effects $R^{-1} = R_{th}^{-1} + R_{iso}^{-1}$.

The bending of a crystal of length l causes the mirror to be tilted by an angle l/R. The tilt results in the reflected ray move by a distance $\delta = 2lL/R$ along the wall located at a distance L.

The response of the crystal to irradiation predicted by the model occurs as follows: when the light is turned on, the curvature of the crystal increases by R_∞^{-1} for a time $\sim t_c$, according to (13). As a result, the laser beam is rapidly shifted to the distance δ_{th}

$$\delta_{th} = 2lL\left(\frac{1}{R}\right)_{\infty}. \tag{17}$$

Simultaneously, the curvature grows at a constant rate determined by eqn (16), causing the beam to shift at a rate of

$$\frac{\mathrm{d}\delta_{iso}}{\mathrm{d}t} = 2lL\frac{\mathrm{d}}{\mathrm{d}t}\left(\frac{1}{R}\right)_{iso}. \tag{18}$$

When the radiation is turned off, the bending achieved by the transformation remains fixed, while the thermal bending disappears in a time $\sim t_c$. The schematic evolution of the total displacement $\delta = \delta_{th} + \delta_{iso}$ is identical to the experimentally observed effect shown in Fig. 2.

The ratio of the rate $d\delta_{iso}/dt$ to δ_{th}, measured in one experiment is independent of the light intensity

$$\frac{1}{\delta_{th}}\frac{d\delta_{iso}}{dt} = 12\varphi\frac{\kappa}{\hbar\omega}\frac{v_0}{h^2}\frac{\varepsilon_0}{\alpha_T}F,$$
$$F = \frac{(\mu h)^3\left(1+e^{-\mu h}\right) - 2(\mu h)^2\left(1-e^{-\mu h}\right)}{[(\mu h)^3 - 12\mu h](1+e^{-\mu h}) + 24(1-e^{-\mu h})}, \quad (19)$$

which makes it possible to determine the quantum yield of the reaction φ using the characteristics of the substance that can be obtained experimentally. The coefficient $F(\mu h)$ varies between 0.833 at $\mu h \gg 1$, and 1 at $\mu h \ll 1$, so that the relative error in the quantum yield will not exceed $\sim$10% in most cases because of the inaccurate value of μ.

Thus, the considered method allows to determine quite accurately the quantum yield of the photochemical reaction in crystals without knowing the value of the light intensity penetrating into the crystal. In addition, the analysis of the photothermal effect can be used as an independent method for determining the thermal conductivity coefficient of various substances, as well as the irradiation intensity.

4 Experimental results

The photothermal effect curves obtained at successive exposures of the 13 mm crystal are shown in Fig. 3, where all data are shifted to the origin for the ease of presentation. The results are jointly analyzed according to the given model, with common values of t_c, δ_{th}, and $d\delta_{iso}/dt$.

The value of t_c was 57 $\pm$ 4 ms for the 280 μm thick crystal, which corresponds to $D_T = 1.4 \times 10^{-7}$ m^2 s^{-1} and $\kappa = 0.43 \pm 0.04$ J m^{-1} K^{-1} (the heat capacity was estimated by the Neumann–Kopp rule as 3×10^6 J m^{-3} K^{-1}). From the value of δ_{th} = 0.7 mm the irradiation power penetrating the crystal in this experiment was evaluated to be J_0 = 17 mW cm^{-2} according to eqn (13) and (17), which corresponds to the photon flux $I_0 = 3.9 \times 10^{16}$ cm^{-2} s^{-1} for a 465 nm LED used in the experiment.

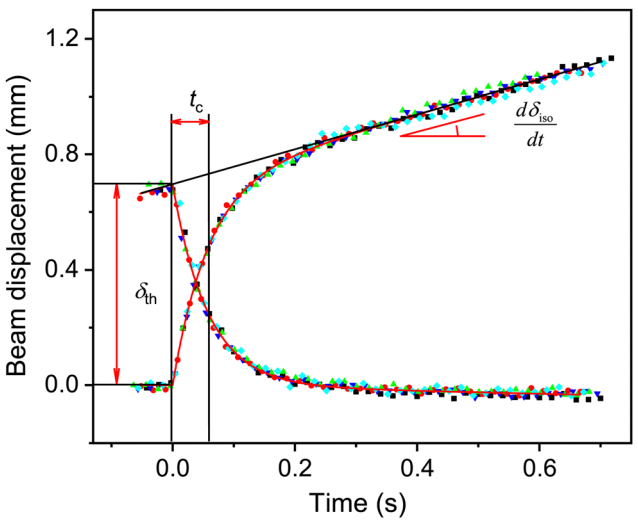

Fig. 3 Photothermal effect at switching the irradiation on and off, corresponding to the data in Fig. 2 shifted to the common origin of coordinates. The dots of different colors correspond to five cycles of the irradiation on and off, the solid line is the fitted analytical model.

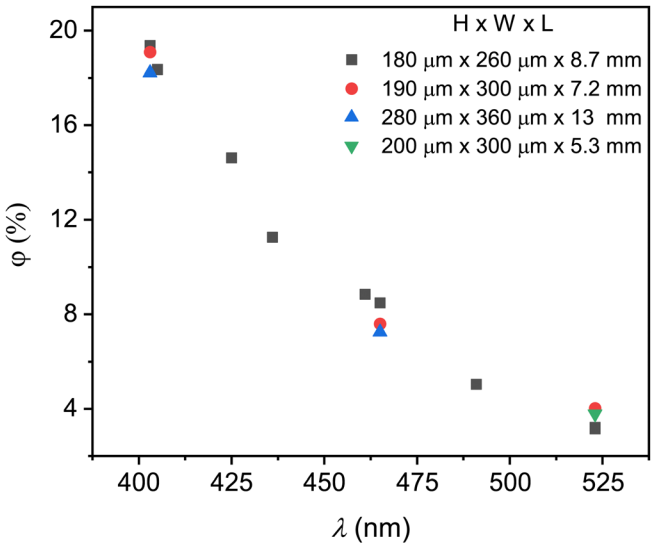

Fig. 4 Wavelength dependence of the quantum yield of isomerization obtained for four different crystals (geometrical dimension thickness × width × length are given in the figure).

The resulting dependence $\varphi(\lambda)$ obtained on different crystals is shown in Fig. 4. The dependence agrees with the data obtained earlier by another method, from the kinetics of photomechanical response of thin crystals, using the values of source intensities measured by the average radiation power in the light field.[21] The method proposed here, however, gives more reliable information due to the independence of the absolute value of the obtained quantum yield from the intensity of the used source, while the use of the average intensity of the light beam can lead up to a 2-fold variation in the determined quantum yield.[20]

The value of $\varphi = 0.2 \pm 0.05$ reported without specifying the wavelength in the only known measurement of the quantum yield of this reaction in $[Co(NH_3)_5NO_2]X_2$ crystals[33] is in agreement with the present result at λ = 403 nm.

For isomerization of the complex in solutions, it was found that the quantum yield is constant $\sim$0.03 at $\lambda > 400$ nm, but increases with the excitation energy up to $\sim$0.2 at λ = 250 nm.[36] The authors explain the obtained dependence by assuming that the reactive intermediates of the isomerization are ligand-to-metal charge-transfer (CT) excited states. At $\lambda < 400$ nm such excited states are formed directly upon light absorption and isomerize before reaching vibrational equilibrium, which leads to an increase in the quantum yield with the excitation energy. At $\lambda > 400$ nm nonreactive excited states are formed initially corresponding to the ligand field (LF) electronic transition which first reach the vibrational relaxed state, and then transform into the CT reactive states by the internal conversion process, thus providing a constant quantum yield in visible light.

The result obtained here shows a qualitative difference in the influence of the near environment on the studied reaction

in solutions and in the crystal. The growth of φ with excitation energy at $\lambda > 400$ nm indicates that, in contrast to the reaction in solution, the isomerization is faster than the vibrational relaxation for LF excited states in crystals. This result also does not exclude that LF states can be directly reactive in crystal environments.

5 Conclusions

This study developed a technique for determining the quantum yield of photochemical reactions in crystals based on the joint analysis of two types of photomechanical effects simultaneously occurring during irradiation of needle crystals: rapid bending with a certain amplitude caused by heating of the crystal by light, and slower monotonic bending caused by photochemical transformation. Since the amplitudes of both effects are proportional to the same light intensity, their ratio is independent of it, which allows us to determine the quantum yield of a photochemical reactions occurring in crystals with zero information about the light intensity. In addition, the analysis of the photothermal effect allows us to determine the light intensity and thermal conductivity of crystals. The latter can be used as a method for measuring the thermal conductivity of various materials.

In this study, the methodology is applied to determine the wavelength dependence of the quantum yield of nitro–nitrito isomerization in $[Co(NH_3)_5NO_2]Cl(NO_3)$ crystals. For the wavelength range 403–523 nm, a monotonic decrease of the quantum yield from φ = 0.19 to φ = 0.04 was obtained, which is qualitatively different from the reaction in solutions, where φ = 0.03 regardless of λ within the same wavelengths. This result shows that new insights into this reaction can be obtained by methods based on the analysis of photomechanical effects.

Conflicts of interest

There are no conflicts to declare.

Acknowledgements

This research was funded by Russian Science Foundation, grant number 22-23-01130.

Notes and references

1 H. Finkelmann, E. Nishikawa, G. G. Pereira and M. Warner, *Phys. Rev. Lett.*, 2001, **87**, 015501.
2 N. K. Nath, M. K. Panda, S. C. Sahoo and P. Naumov, *CrystEngComm*, 2014, **16**, 1850–1858.
3 P. Commins, I. T. Desta, D. P. Karothu, M. K. Panda and P. Naumov, *Chem. Commun.*, 2016, **52**, 13941–13954.
4 L. Zhu, F. Tong, R. O. Al-Kaysi and C. J. Bardeen, in *Photomechanical Effects in Photochromic Crystals*, ed. T. J. White, Wiley, 2017, pp. 233–274.
5 P. Naumov, S. Chizhik, M. K. Panda, N. K. Nath and E. Boldyreva, *Chem. Rev.*, 2015, **115**, 12440–12490.
6 P. Naumov, D. P. Karothu, E. Ahmed, L. Catalano, P. Commins, J. Mahmoud Halabi, M. B. Al-Handawi and L. Li, *J. Am. Chem. Soc.*, 2020, **142**, 13256–13272.
7 P. Commins, A. Natarajan, C.-K. Tsai, S. I. Khan, N. K. Nath, P. Naumov and M. A. Garcia-Garibay, *Cryst. Growth Des.*, 2015, **15**, 1983–1990.
8 Y. Nakagawa, M. Morimoto, N. Yasuda, K. Hyodo, S. Yokojima, S. Nakamura and K. Uchida, *Chem. – Eur. J.*, 2019, **25**, 7874–7880.
9 D. Kitagawa, R. Tanaka and S. Kobatake, *Phys. Chem. Chem. Phys.*, 2015, **17**, 27300–27305.
10 A. Hirano, D. Kitagawa and S. Kobatake, *CrystEngComm*, 2019, **21**, 2495–2501.
11 D. Kitagawa and S. Kobatake, *J. Phys. Chem. C*, 2013, **117**, 20887–20892.
12 T. Kim, L. Zhu, L. J. Mueller and C. J. Bardeen, *J. Am. Chem. Soc.*, 2014, **136**, 6617–6625.
13 F. Terao, M. Morimoto and M. Irie, *Angew. Chem., Int. Ed.*, 2012, **51**, 901–904.
14 D. Kitagawa and S. Kobatake, *Chem. Commun.*, 2015, **51**, 4421–4424.
15 R. Chandrasekar, *Small*, 2021, **17**, 2100277.
16 M. G. Kuzyk and N. J. Dawson, *Adv. Opt. Photonics*, 2020, **12**, 847–1011.
17 J. Mahmoud Halabi, E. Ahmed, S. Sofela and P. Naumov, *Proc. Natl. Acad. Sci. U. S. A.*, 2021, **118**, e2020604118.
18 E. V. Boldyreva, A. A. Sidelnikov, A. P. Chupakhin, N. Z. Lyakhov and V. V. Boldyrev, *Dokl. Akad. Nauk SSSR*, 1984, **277**, 893–896.
19 E. V. Boldyreva and A. A. Sidelnikov, *Izv. Sib. Otd. Akad. Nauk SSSR, Ser. Khim. Nauk*, 1987, **5**, 139–144.
20 S. Chizhik, A. Sidelnikov, B. Zakharov, P. Naumov and E. Boldyreva, *Chem. Sci.*, 2018, **9**, 2319–2335.
21 E. Ahmed, S. Chizhik, A. Sidelnikov, E. Boldyreva and P. Naumov, *Inorg. Chem.*, 2022, **61**, 3573–3585.
22 A. A. Sidelnikov, S. A. Chizhik, B. A. Zakharov, A. P. Chupakhin and E. V. Boldyreva, *CrystEngComm*, 2016, **18**, 7276–7283.
23 S. Chizhik, P. Gribov, V. Kovalskii and A. Sidelnikov, *Appl. Sci.*, 2022, **12**, 12007.
24 S. Hasebe, Y. Hagiwara, K. Takechi, T. Katayama, A. Furube, T. Asahi and H. Koshima, *Chem. Mater.*, 2022, **34**, 1315–1324.
25 B. Adell, *Z. Anorg. Allg. Chem.*, 1952, **271**, 49–64.
26 V. Balzani, R. Ballardini, N. Sabbatini and L. Moggi, *Inorg. Chem.*, 1968, **7**, 1398–1404.
27 M. Kubota and S. Ohba, *Acta Crystallogr., Sect. B: Struct. Sci.*, 1992, **48**, 627–632.
28 I. Grenthe and E. Nordin, *Inorg. Chem.*, 1979, **18**, 1869–1874.
29 A. M. Heyns and D. de Waal, *Spectrochim. Acta, Part A*, 1989, **45**, 905–909.
30 N. Masciocchi, A. Kolyshev, V. Dulepov, E. Boldyreva and A. Sironi, *Inorg. Chem.*, 1994, **33**, 2579–2585.
31 W. W. Wendlandt and J. H. Woodlock, *J. Inorg. Nucl. Chem.*, 1965, **27**, 259–260.

32 B. Adell, *Z. Anorg. Allg. Chem.*, 1955, **279**, 219–224.
33 E. Rose and D. McClure, *J. Photochem.*, 1981, **17**, 171.
34 C. A. Schneider, W. S. Rasband and K. W. Eliceiri, *Nat. Methods*, 2012, **9**, 671–675.
35 W. Kays, M. Crawford and B. Weigand, *Convective Heat and Mass Transfer*, McGraw-Hill, 2005.
36 F. Scandola, C. Bartocci and M. A. Scandola, *J. Phys. Chem.*, 1974, **78**, 572–575.